

## Rim-Functionalized Cryptophane-111 Derivatives via Heterocapping, and their Xenon Complexes

Akil I. Joseph, Gracia El-Ayle, Céline Boutin, Estelle Léonce, Patrick Berthault, and K. Travis Holman\*  
Email: kth7@georgetown.edu

### Table of Contents

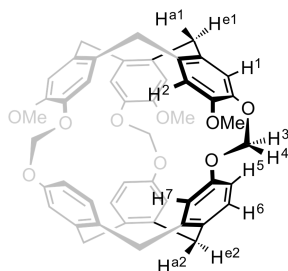
<b>1. Materials and methods</b> .....	<b>2</b>
<b>2. Syntheses</b> .....	<b>2</b>
<b>2.1. Synthesis of compound (±)-trimethoxy-cryptophane-111 ((MeO)<sub>3</sub>-111, C<sub>48</sub>H<sub>42</sub>O<sub>9</sub>)</b> .....	<b>2</b>
<b>2.2. Synthesis of compound (±)-tribromo-cryptophane-111 (Br<sub>3</sub>-111, C<sub>45</sub>H<sub>33</sub>Br<sub>3</sub>O<sub>6</sub>)</b> .....	<b>3</b>
<b>2.3. Failed regioselective bromination of 3-methoxybenzyl alcohol</b> .....	<b>4</b>
<b>3. Electrospray Mass Spectra</b> .....	<b>5</b>
<b>4. NMR spectroscopy</b> .....	<b>6</b>
<b>4.1. Production of laser-polarized xenon</b> .....	<b>10</b>
<b>5. X-ray crystallography</b> .....	<b>12</b>
<b>5.1. Growth of X-ray quality crystals</b> .....	<b>12</b>
<b>5.2. Data collection and structure determination</b> .....	<b>12</b>
<b>5.3. Cavity volumes</b> .....	<b>12</b>
<b>5.4. (MeO)<sub>3</sub>-111·1.5DCE and 0.92Xe@((MeO)<sub>3</sub>-111·1.5DCE</b> .....	<b>13</b>
<b>5.5. 1.5[(MeO)<sub>3</sub>-111]·NO<sub>2</sub>Me</b> .....	<b>15</b>
<b>5.6. Br<sub>3</sub>-111 and Xe@Br<sub>3</sub>-111</b> .....	<b>17</b>
<b>6. References</b> .....	<b>23</b>

## 1. Materials and methods.

Reagents were obtained from Sigma-Aldrich while solvents were obtained from Alfa Aesar, both reagent and solvent were of reagent grade purity. The silica gel (40–60  $\mu\text{m}$ , *SiliaFlash*®) was obtained from SILICYCL while the thin-layer chromatography (TLC, 1000  $\mu\text{m}$ , *UNIPLATE*™) plates were obtained from ANALTECH. Xenon gas was purchased from GTS-Welco. All reactions were done under  $\text{N}_2$  atmosphere using standard Schlenk techniques. Standard  $^1\text{H}$  (400 MHz) and  $^{13}\text{C}$  (100 MHz) NMR spectra were carried out on a Varian 400-MR spectrometer, unless otherwise indicated. Unless otherwise indicated, chemical shifts given are based on the residual solvent peaks. Splitting patterns are labeled as singlet (s), doublet (d), triplet (t) and broad (br.). ESI-MS data were obtained using Varian 500 MS spectrometer running in positive ion mode. ESI-MS masses were calculated by mMass software suite.<sup>S1</sup> Encapsulated species are indicated by the @ symbol. **3a**,<sup>S2, S3</sup> **3b**,<sup>S4</sup> and **3c**<sup>S5</sup> were synthesized by literature methods.

## 2. Syntheses.

### 2.1. Synthesis of compound ( $\pm$ )-trismethoxy-cryptophane-111 ((MeO)<sub>3</sub>-111, C<sub>48</sub>H<sub>42</sub>O<sub>9</sub>).

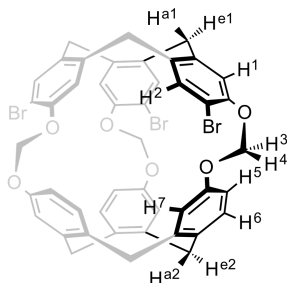


$$\text{fw} = 762 \text{ g} \cdot \text{mol}^{-1}$$

( $\pm$ )-Cyclotriphenolene (CTP or **3a**, 58 mg, 0.18 mmol) and ( $\pm$ )-cyclotriguaiacylene (CTG or **3c**, 223 mg, 0.55 mmol) were placed with  $\text{Cs}_2\text{CO}_3$  (2.66 g, 10.00 mmol) in anhydrous DMF (9 mL). The mixture was allowed to stir at 75  $^\circ\text{C}$  for an hour.  $\text{BrCH}_2\text{Cl}$  (30 mL, 449 mmol) was added and the mixture was then left at 75  $^\circ\text{C}$  overnight. The solvent was removed at 80  $^\circ\text{C}$  under vacuum. The solid remaining was sonicated with  $\text{CHCl}_3$  ( $2 \times 30$  mL) then filtered through a pad of silica (10 mL) and eluted with  $\text{CH}_2\text{Cl}_2$ . The eluent was collected and washed with brine and deionized water. The organic layer was dried with anhydrous  $\text{MgSO}_4$ , and the solvent was removed under vacuum to give a yellow solid. This material was chromatographed on a preparative TLC plate with a mobile phase of  $\text{CHCl}_3$ . The silica fraction with absorbed (**MeO**)<sub>3</sub>-111 ( $R_f = 0.35$ ) was collected and eluted with  $\text{CHCl}_3$  to remove the compound. The

solvent was removed under vacuum to give an off-white solid (25 mg, yield 18%).  $^1\text{H}$  NMR (400 MHz,  $\text{CDCl}_3$ ,  $\delta$ , see figure above for labels): 6.94 (d,  $J = 8.0$  Hz, 3H,  $\text{H}^6$ ), 6.91 (s, 3H,  $\text{H}^1$ ), 6.80 (br. s, 3H,  $\text{H}^7$ ), 6.63 (s, 3H,  $\text{H}^2$ ), 6.52 (d,  $J = 8.0$  Hz, 3H,  $\text{H}^5$ ), 5.93 (d,  $J = 6.8$  Hz, 3H,  $\text{H}^3$ ), 5.68 (d,  $J = 6.8$  Hz, 3H,  $\text{H}^4$ ), 4.47 (d,  $J = 13.8$  Hz, 3H,  $\text{H}^{\text{a}2}$ ), 4.43 (d,  $J = 13.5$  Hz, 3H,  $\text{H}^{\text{a}1}$ ), 4.00 (s, 9H, OMe), 3.35 (d,  $J = 13.8$  Hz, 3H,  $\text{H}^{\text{e}2}$ ), 3.31 (d,  $J = 13.5$  Hz, 3H,  $\text{H}^{\text{e}1}$ ).  $^{13}\text{C}$  NMR (100 MHz,  $\text{CDCl}_3$ ,  $\delta$ ): 155.22, 148.33, 144.00, 140.40, 134.41, 132.55, 131.89, 130.51, 120.28, 116.03, 114.99, 114.63, 92.57, 56.93, 36.25, 36.19. ESI-MS ( $m/z$ ) (MeOH, CsCl added): calculated for  $(\text{C}_{48}\text{H}_{45}\text{O}_{10}, [\text{H}_3\text{O}@(\text{MeO})_3\text{-111}]^+)$ : 780.4 found 780.4, calculated for  $[\text{C}_{48}\text{H}_{42}\text{O}_9\text{Cs}]^+$ : 895.2 found 895.2. Decomposes over 250 °C.

## 2.2. Synthesis of compound ( $\pm$ )-trisbromo-cryptophane-111 (**Br<sub>3</sub>-111**, $\text{C}_{45}\text{H}_{33}\text{Br}_3\text{O}_6$ ).



fw = 909  $\text{g}\cdot\text{mol}^{-1}$

**Br<sub>3</sub>-111** was synthesized and isolated following the procedure outlined for the synthesis of **(MeO)<sub>3</sub>-111** using **CTP** or **3a** (38 mg, 0.12 mmol), ( $\pm$ )-trisbromo-cyclotriphenolene (**Br<sub>3</sub>-CTP** or **3b**, 200 mg, 0.36 mmol), DMF (9 mL),  $\text{Cs}_2\text{CO}_3$  (2.28 g, 7.00 mmol) and  $\text{BrCH}_2\text{Cl}$  (30 mL, 449 mmol). However, the mixture was initially stirred for two hours at 75 °C before the addition of  $\text{BrCH}_2\text{Cl}$ . The yellow solid collected was loaded on a silica column and chromatographed using  $\text{CHCl}_3$  ( $R_f = 0.57$ ,  $\text{CH}_2\text{Cl}_2$ ). The solvent was removed under vacuum to give **Br<sub>3</sub>-111** as a white solid (18.4 mg, 17 %). The product contains traces of the homodimeric product **Br<sub>6</sub>-111** (~2%).  $^1\text{H}$  NMR (400 MHz,  $\text{CD}_2\text{Cl}_2$ ,  $\delta$ , see figure above for labels): 7.15 (s, 3H,  $\text{H}^2$ ), 7.06 (d, 3H,  $J = 8.0$  Hz,  $\text{H}^6$ ), 6.86 (s, 3H,  $\text{H}^1$ ), 6.79 (d, 3H,  $J = 2.4$  Hz,  $\text{H}^7$ ), 6.69 (d, 3H,  $J = 8.0$  Hz,  $J = 2.4$  Hz,  $\text{H}^5$ ), 5.84 (d, 3H,  $J = 8.0$  Hz,  $\text{H}^3/\text{H}^4$ ), 5.72 (d, 3H,  $J = 8.0$  Hz,  $\text{H}^3/\text{H}^4$ ), 4.42 (d, 3H,  $J = 13.4$  Hz,  $\text{H}^{\text{a}2}$ ), 4.30 (d, 3H,  $J = 14.0$  Hz,  $\text{H}^{\text{a}1}$ ), 3.30 (d, 3H,  $J = 13.4$  Hz,  $\text{H}^{\text{e}2}$ ), 3.25 (d, 3H,  $J = 14.0$  Hz,  $\text{H}^{\text{e}1}$ ). ESI-MS ( $m/z$ ) calculated for  $(\text{C}_{45}\text{H}_{36}\text{Br}_3\text{O}_7, [\text{H}_3\text{O}@(\text{Br}_3\text{-111})^+)$ : 926.7, found: 927.0. Decomposes over 300 °C. Note that analysis of the crude reaction mixture by ESI-MS ( $m/z$ ) showed

traces of the ( $\pm$ )-hexabromo-cryptophane-111 derivative **Br<sub>6</sub>-111**; calculated for [C<sub>45</sub>H<sub>30</sub>Br<sub>6</sub>O<sub>6</sub>Cs]<sup>+</sup>: 1278.6, found: 1278.1.

### 2.3. Failed regioselective bromination of 3-methoxybenzyl alcohol.

( $\pm$ )-Trisbromocyclotriphenolene (**3b**) was previously synthesized by Collet and coworkers in five steps.<sup>S4</sup> In the first three steps, 3-hydroxybenzoic acid is brominated using Br<sub>2</sub>, methylated using dimethyl sulfate, and subsequently reduced using lithium aluminum hydride to give 4-bromo-3-methoxybenzyl alcohol (**1b**) in 24% overall yield. A recent publication by Speicher *et al.* reported an appealing, single-step, high yield (88%) synthesis of 4-bromo-3-methoxybenzyl alcohol (**1b**) by regioselective bromination of commercially available 3-methoxybenzyl alcohol, suggesting that the overall synthesis of **3b** can be shortened considerably and that **3b** ought to now be more accessible in larger quantities. In our hands, however, the Speicher procedure yielded almost exclusively the 2-bromo-5-methoxybenzyl alcohol isomer. The <sup>1</sup>H NMR spectrum of our isolated product (2-bromo-5-methoxybenzyl alcohol, as it turns out) is consistent with that reported by Speicher as purportedly being **1b**. Moreover, the Speicher product is isolated as an oil whereas the melting point of authentic **1b** is reported to be ~100 °C. Furthermore, our 2-bromo-5-methoxybenzyl alcohol product from the Speicher procedure could not be successfully cyclized to **2b**. For comparison, an authentic sample of **1b** was prepared by the three-step method above; this product readily cyclizes to give **2b**. The identities of the isomeric compounds were unequivocally established by 1D <sup>1</sup>H-<sup>1</sup>H NOESY studies, as shown below.

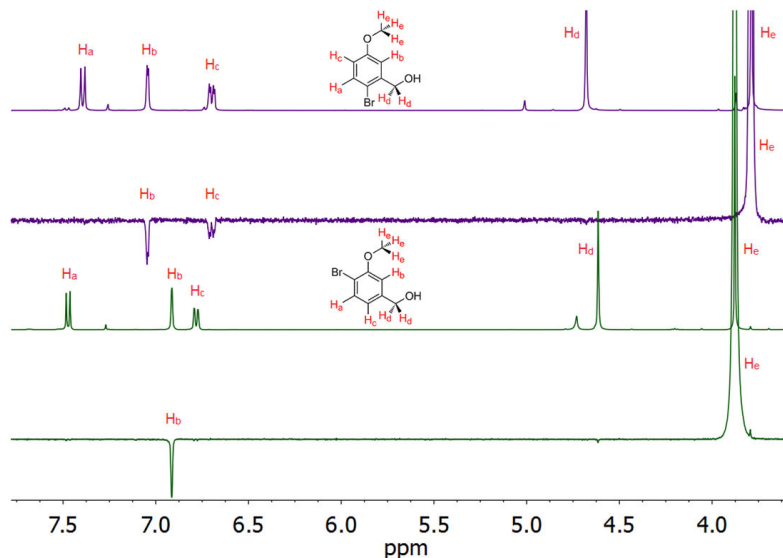


**Figure S1.**  $^1\text{H}$  NMR spectrum (top) and the corresponding 1D  $^1\text{H}$ - $^1\text{H}$  NOESY spectrum (bottom) of 2-bromo-5-methoxybenzyl alcohol obtained from the direct bromination of 3-methoxybenzyl alcohol according to the method of Speicher *et al.* (purple) and an authentic sample of 4-bromo-3-methoxybenzyl alcohol obtained from the three-step synthesis reported by Collet and coworkers (green). In the  $^1\text{H}$ - $^1\text{H}$  NOESY spectra, the methyl peaks  $\text{H}_c$  were saturated and showed through-space interaction with both  $\text{H}_b$  and  $\text{H}_d$  for 2-bromo-5-methoxybenzyl alcohol and with only  $\text{H}_b$  for 4-bromo-3-methoxybenzyl alcohol. All spectra were recorded in  $\text{CDCl}_3$  at 298 K.

### 3. Electrospray Mass Spectra.

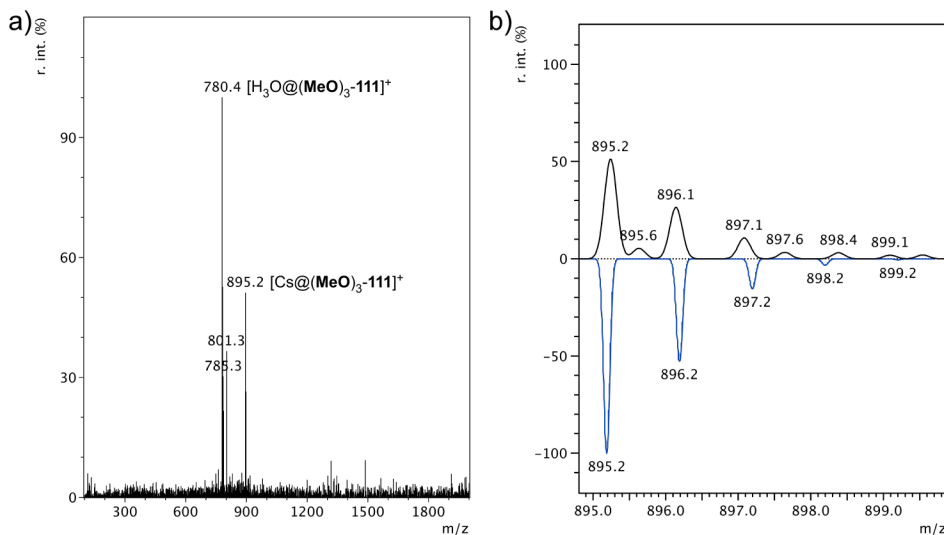


**Figure S2.** (a) ESI-MS spectrum (methanol, CsCl added) of  $(\text{MeO})_3\text{-111}$ . The peak at 780.4 m/z corresponds to  $[\text{H}_3\text{O}@\text{(MeO)}_3\text{-111}]^+$ , 780.4 calc. The peak at 785.3 m/z corresponds to  $[\text{Na}@\text{(MeO)}_3\text{-111}]^+$ , 785.3 calc. The peak at 801.3 m/z corresponds to  $[\text{K}@\text{(MeO)}_3\text{-111}]^+$ , 801.2 calc. (b) The peak of  $[\text{Cs}@\text{(MeO)}_3\text{-111}]^+$  is shown, 895.2 m/z calculated vs. 895.2 m/z experimental for major peak. The experimental data is shown in black versus calculated shown in blue.

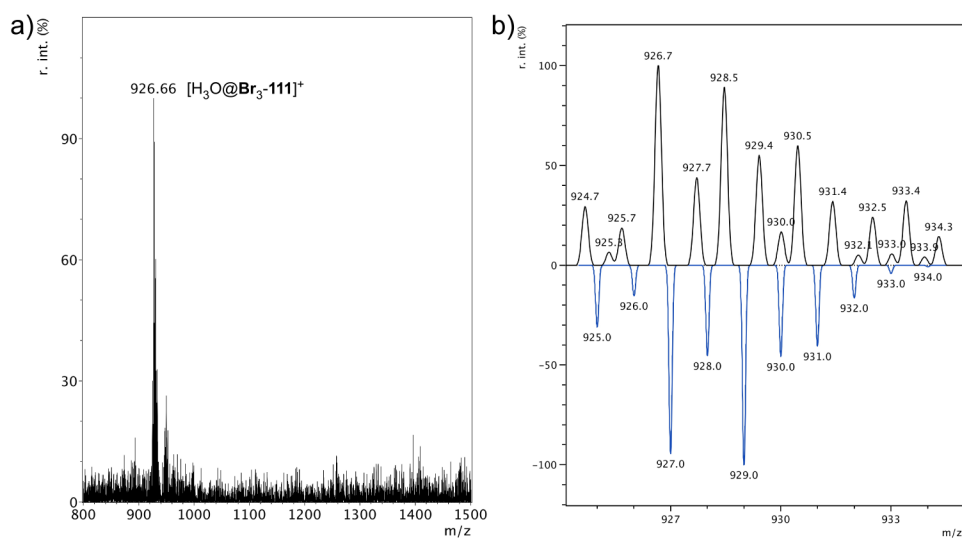


**Figure S3.** (a) ESI-MS spectrum (methanol) of  $\text{Br}_3\text{-111}$ . (b) The peak of  $[\text{H}_2\text{O}@\text{Br}_3\text{-111}]^+$  is shown, 926.7 m/z calculated vs. 927.0 m/z experimental for major peak. The experimental data is shown in black versus calculated shown in blue.

#### 4. NMR spectroscopy.

The following  $^1\text{H}$  (400 MHz) and  $^{13}\text{C}$  (100 MHz) NMR spectra were carried out on a Varian 400-MR spectrometer.

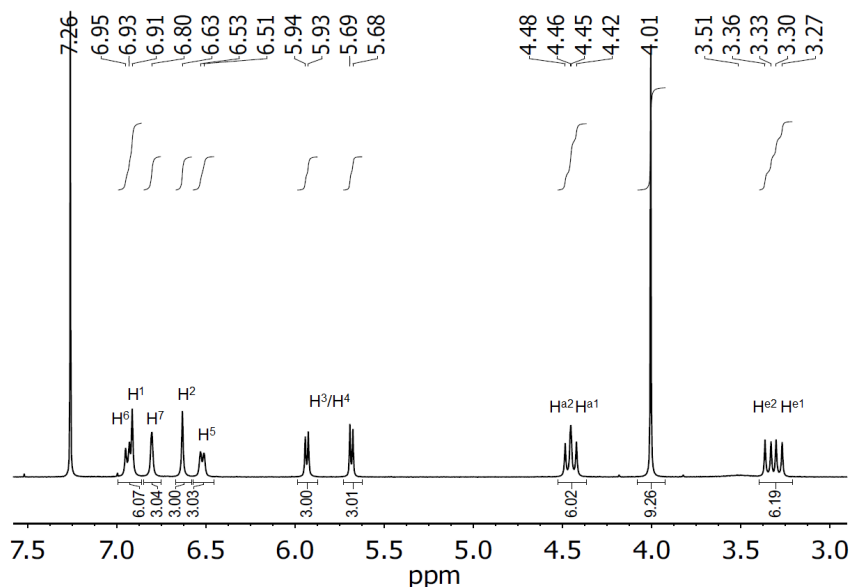


**Figure S4.**  $^1\text{H}$  NMR spectrum ( $\text{CDCl}_3$ , 298 K) of  $(\text{MeO})_3\text{-111}$  (0.87 mM). Labels correspond to the structure drawn in Section 2.1 above.

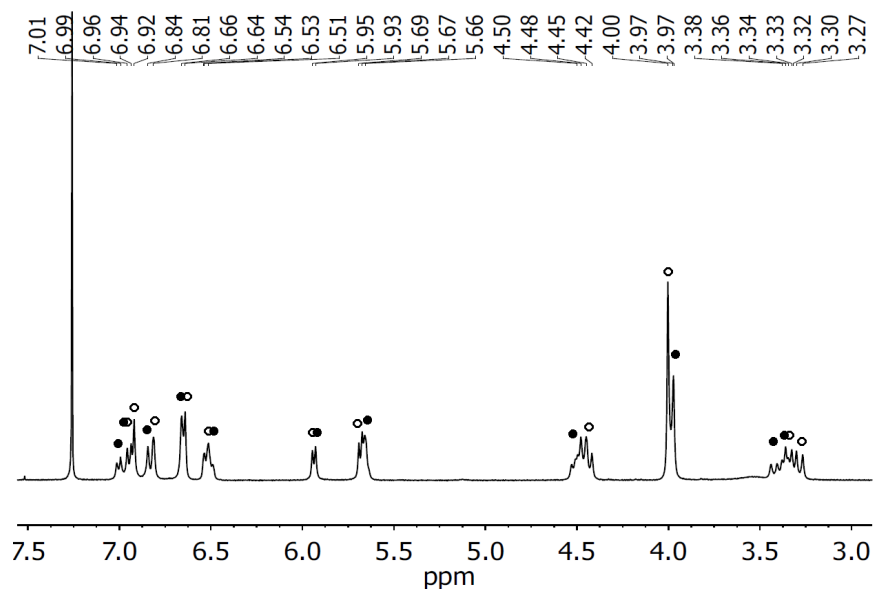


**Figure S5.**  $^1\text{H}$  NMR spectrum ( $\text{CDCl}_3$ , 298 K) of the sample of  $(\text{MeO})_3\text{-111}$  from above, but after saturation of the solution with xenon ( $\sim 200$  mM). Black circles correspond to the signals of the  $\text{Xe}@(\text{MeO})_3\text{-111}$  complex and guest-free  $(\text{MeO})_3\text{-111}$  and is indicated by open circles.

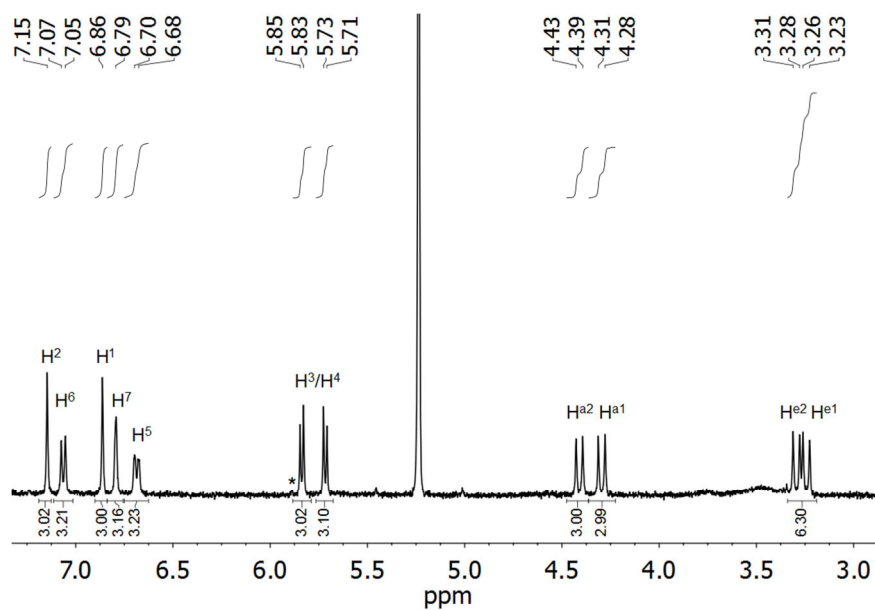


**Figure S6.**  $^1\text{H}$  NMR spectrum ( $\text{CD}_2\text{Cl}_2$ , 298 K) of  $\text{Br}_3\text{-111}$ . The asterisk (\*) is the  $\text{Br}_6\text{-111}$  impurity. Labels correspond with the chemical structure in Section 2.2 above

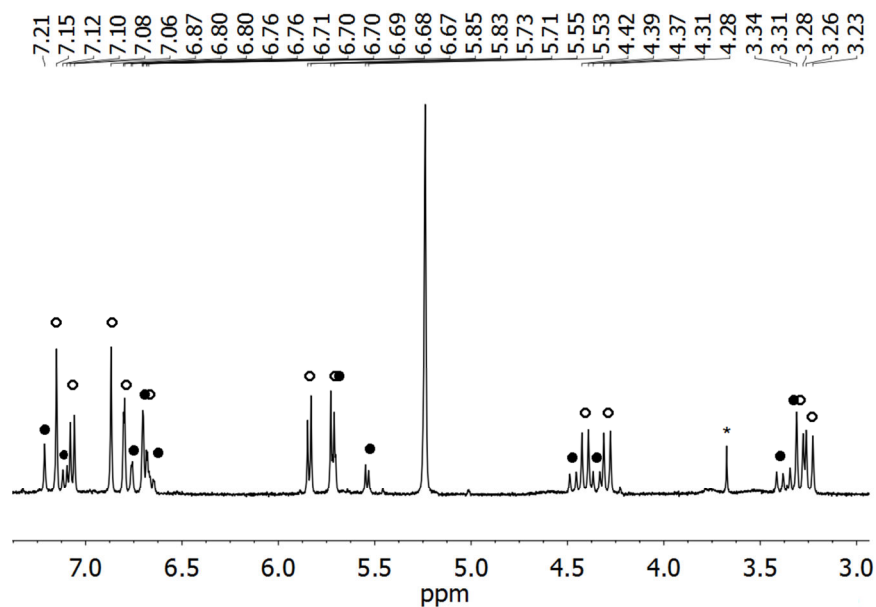


**Figure S7.**  $^1\text{H}$  NMR spectrum ( $\text{CD}_2\text{Cl}_2$ , 298 K) of the sample of **Br<sub>3</sub>-111** from above, but after saturation of the solution with xenon. Black circles correspond to the signals of the  $\text{Xe}@\text{Br}_3\text{-111}$  complex and guest-free **Br<sub>3</sub>-111** is indicated by open circles. The asterisk (\*) corresponds to a signal from an impurity in the xenon.

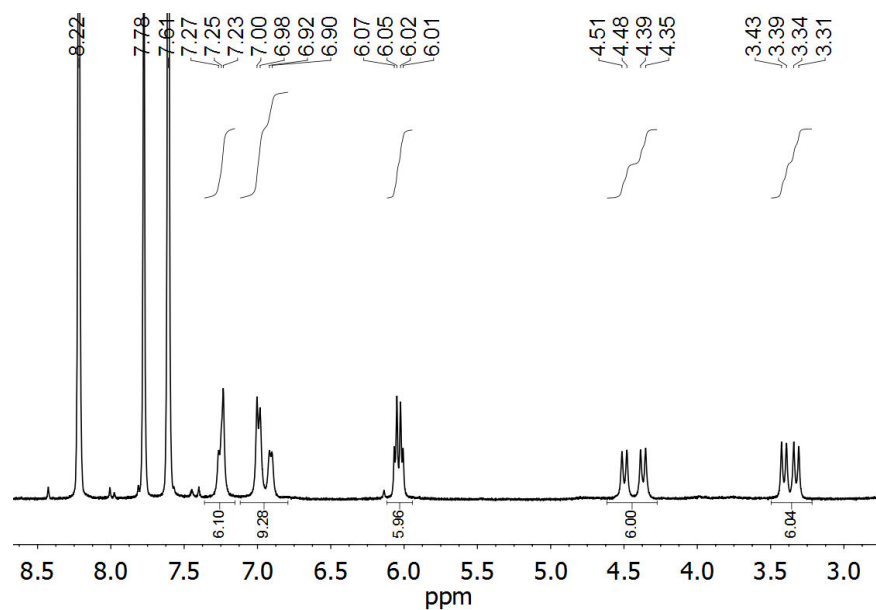


**Figure S8.**  $^1\text{H}$  NMR spectrum ( $\text{C}_6\text{D}_5\text{NO}_2$ , 298 K) of **Br<sub>3</sub>-111** (0.46 mM). The tiny signal at 6.1 ppm is the **Br<sub>6</sub>-111** impurity.

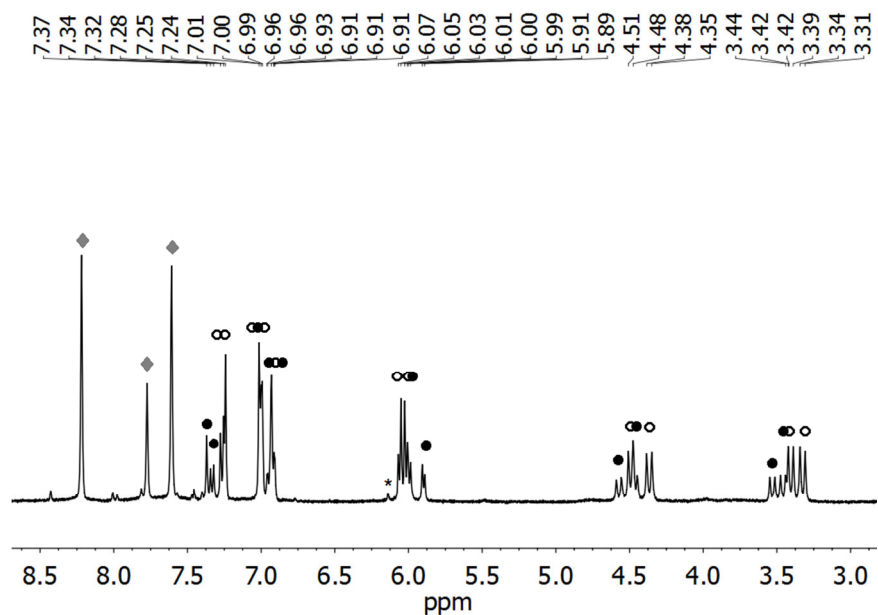


**Figure S9.**  $^1\text{H}$  NMR spectrum ( $\text{C}_6\text{D}_5\text{NO}_2$ , 298 K) of the sample of **Br<sub>3</sub>-111** from above, but after saturation of the solution with xenon ( $\sim 57$  mM). Black circles correspond to the signals of the  $\text{Xe}@\text{Br}_3\text{-111}$  complex and guest-free **Br<sub>3</sub>-111** is indicated by open circles. The difference between the intensities of the residual solvent peaks between the two spectra is due to a shorter delay time between scans employed in acquiring this spectrum. The asterisk (\*) denotes the **Br<sub>6</sub>-111** impurity.

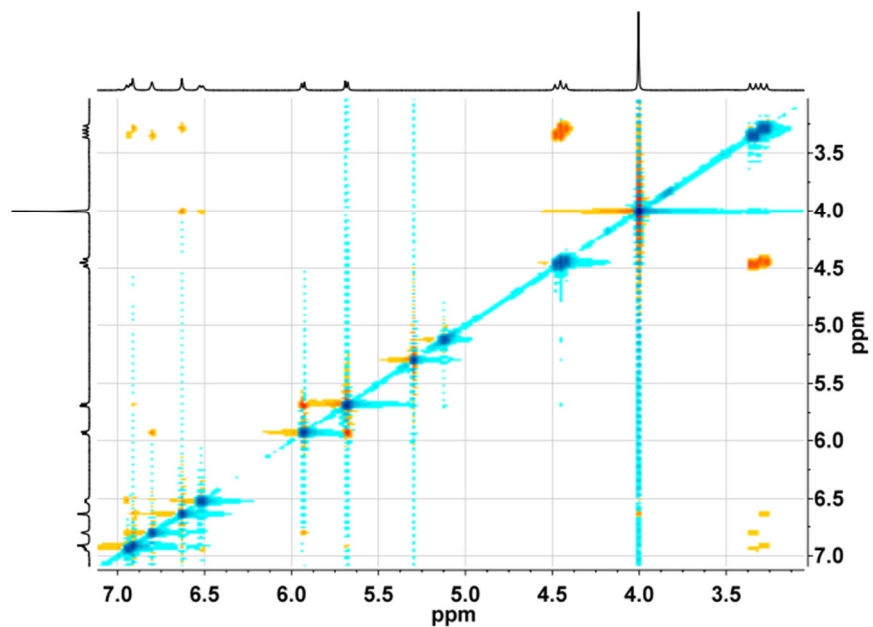


**Figure S10.** 2D  $^1\text{H}$ - $^1\text{H}$  ROESY spectrum ( $\text{CDCl}_3$ , 298 K) of **(MeO)<sub>3</sub>-111**.

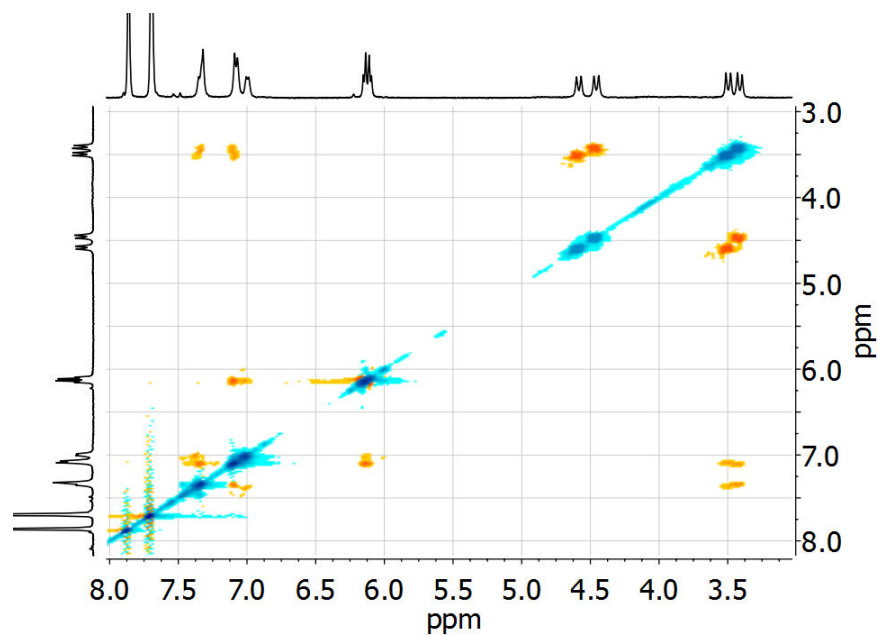


**Figure S11.** 2D  $^1\text{H}$ - $^1\text{H}$  ROESY spectrum ( $\text{CD}_2\text{Cl}_2$ , 298 K) of **Br<sub>3</sub>-111**.

#### 4.1. Production of laser-polarized xenon

A home-built optical pumping setup using a 5W Titanium:Sapphire laser was described in references S6 and S7.<sup>S6, S7</sup> It provides an average xenon polarization of 40% (measured on the gas phase in the spectrometer). Hyperpolarized xenon frozen into a cold finger was transported inside a 3 kG solenoid. The transfer from this cold finger to the NMR tube was made via a simple Joule-Gay Lussac expansion in the fringe field of the magnet in order to preserve polarization. Vigorous shaking of the tube followed by a 10s wait time before each hyperpolarized  $^{129}\text{Xe}$  NMR experiment ensured homogenization of the sample after disappearance of the bubbles.

The  $^{129}\text{Xe}$  experiments designed to study the interaction between xenon and the cryptophane were carried out on a Bruker Avance II 500 spectrometer equipped with 5 mm HNX and Broadband inverse probeheads. Accurate calibration of the temperature was made using a methanol sample. Prior the introduction of the hyperpolarized noble gas, the solutions were degassed using several freeze-pump-thaw cycles.

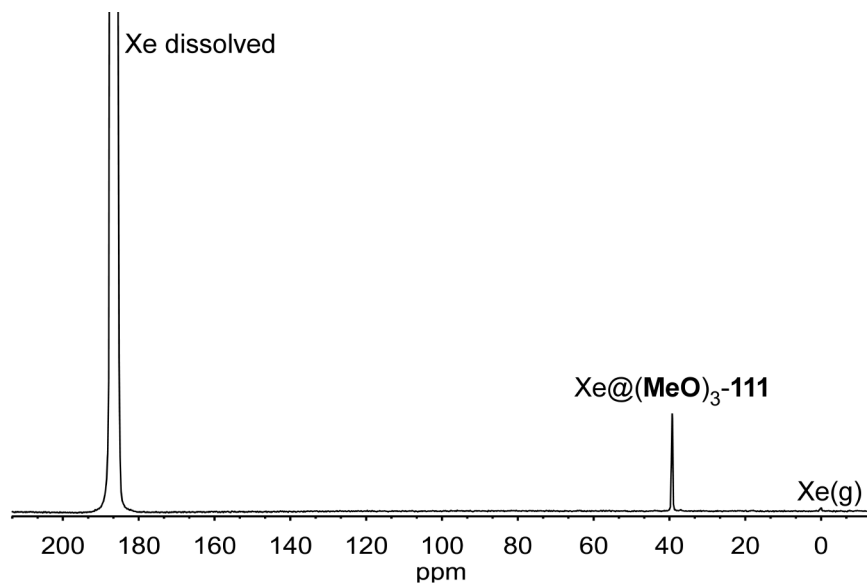


**Figure S12.**  $^{129}\text{Xe}$  NMR spectrum ( $\text{CDCl}_3$ , 293 K) of a solution of **(MeO)<sub>3</sub>-111** (0.66 mM total) after saturation of the solution with 25.5 torr of hyperpolarized xenon. Chemical shifts are referenced to the  $\text{Xe(g)}$  peak at 0 ppm. The  $\text{Xe}@(\text{MeO})_3\text{-111}$  species is clearly observed at 39.3 ppm.

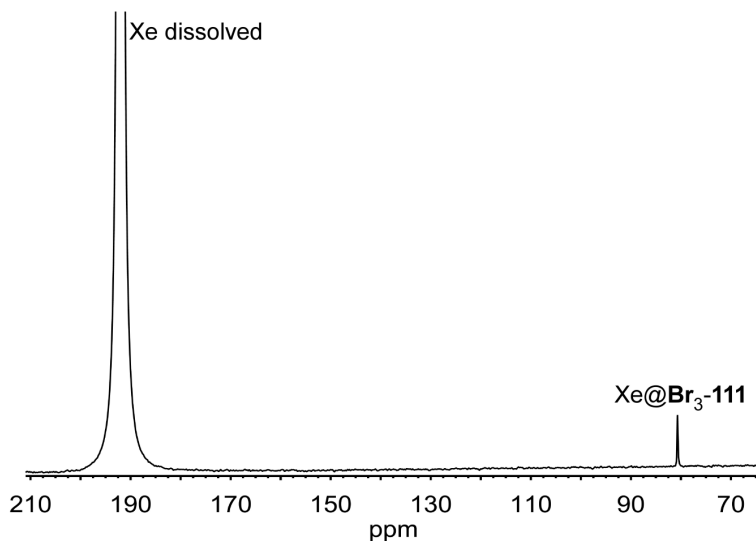


**Figure S13.**  $^{129}\text{Xe}$  NMR spectrum ( $\text{CD}_2\text{Cl}_2$ , 293 K) of a solution of **Br<sub>3</sub>-111** (0.48 mM total) after saturation of the solution with 10.7 torr of hyperpolarized xenon. Chemical shifts are referenced to the dissolved xenon peak (192 ppm in  $\text{CD}_2\text{Cl}_2$ ). The  $\text{Xe}@Br_3\text{-111}$  species is clearly observed at 80.7 ppm.

## 5. X-ray crystallography

### 5.1. Growth of X-ray quality crystals

Crystals of  $(\text{MeO})_3\text{-111}\cdot 1.5\text{DCE}$  were grown by slow evaporation of a solution of  $(\text{MeO})_3\text{-111}$  in 1,2-dichloroethane (DCE) at room temperature. Crystals of  $1.5[(\text{MeO})_3\text{-111}]\cdot \text{NO}_2\text{Me}$  and  $\text{Br}_3\text{-111}$  were grown by heating and cooling to room temperature supersaturated solutions of the appropriate cryptophane in nitromethane ( $\text{NO}_2\text{Me}$ ) or nitrobenzene ( $\text{NO}_2\text{Ph}$ ), respectively.  $\text{Xe@cryptophane}$  crystals were grown in a sealed pressurized vessel over a period of one week.  $0.92\text{Xe}@(\text{MeO})_3\text{-111}\cdot 1.5\text{DCE}$  crystals were obtained from a saturated solution of  $(\text{MeO})_3\text{-111}$  in DCE under a pressure of 14 bars of  $\text{Xe(g)}$  whereas  $0.96\text{Xe}@(\text{Br}_3\text{-111})$  crystals were grown from a saturated solution of  $\text{Br}_3\text{-111}$  in  $\text{NO}_2\text{Ph}$  under a pressure of 17 bars of  $\text{Xe(g)}$ .

### 5.2. Data collection and structure determination

Single crystal X-ray diffraction data of  $(\text{MeO})_3\text{-111}\cdot 1.5\text{DCE}$ ,  $1.5[(\text{MeO})_3\text{-111}]\cdot \text{NO}_2\text{Me}$ , and  $\text{Br}_3\text{-111}$  were collected on a Siemens SMART three-circle X-ray diffractometer while  $0.92\text{Xe}@(\text{MeO})_3\text{-111}\cdot 1.5\text{DCE}$  and  $0.96\text{Xe}@(\text{Br}_3\text{-111})$  were collected on a Bruker APEX II Duo, both diffractometers were equipped with an APEX II CCD detector (Bruker-AXS). All X-ray diffraction data was collected at 100(2) K using an Oxford Cryosystems 700 Cryostream, using Mo K $\alpha$  radiation (0.71073 Å). The crystal structures were solved by direct methods using SHELXS, and all structural refinements were conducted using SHELXL-97-2.<sup>S8</sup> With the exception of some included disordered moieties, all non-hydrogen atoms were modeled with anisotropic displacement parameters. All hydrogen atoms were placed in calculated positions and were refined using a riding model with coordinates and isotropic displacement parameters being dependent upon the atom to which they are attached. The program X-Seed was used as a graphical interface for the SHELX software suite and for the generation of figures.<sup>S9</sup> CCDC deposition numbers 935199, 1027976, 1027977, 1027974, and 1027975 contain the supplementary crystallographic data for the single crystal structures reported here. These data can be obtained free of charge from The Cambridge Crystallographic Data Centre via [www.ccdc.cam.ac.uk/data\\_request/cif](http://www.ccdc.cam.ac.uk/data_request/cif).

### 5.3. Cavity volumes

Cavity volumes are commonly extracted from atomic coordinate data by computationally probing the cavity with a sphere of a defined probe radius. The volume of space that can be encompassed by rolling

the sphere around the interior of the cavity is summed over all achievable positions of the sphere, considering the van der Waals radii of the atoms. For the cryptophane cavity volumes described herein, crystal structure data were used and, prior to the calculation, all C-H bonds were normalized to 1.09 Å. Cavity volumes were calculated using the MS-Roll interface of X-Seed, employing the default van der Waals atomic radii and a probe sphere with a radius of 1.4 Å. The following default van der Waals radii were used: C = 1.70 Å, H = 1.20 Å, O = 1.52 Å, Br = 1.93 Å, and Xe = 2.16 Å. The cavities shown were imaged using the X-Seed software.

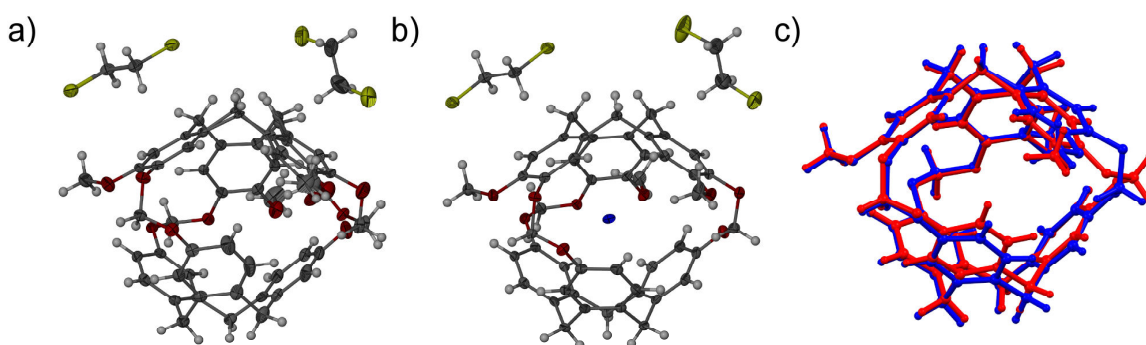


**Figure S14.** Thermal ellipsoid plots (60% probability) of the crystal structures (a)  $(\text{MeO})_3\text{-111}\cdot 1.5\text{DCE}$ ; both disordered conformations are shown. For the major (65%) occupancy (more closed) conformer of the disordered species:  $l = 7.7 \text{ \AA}$ ,  $\theta = 56(2)^\circ$ ,  $V_c \approx 42 \text{ \AA}^3$ ; (b)  $\text{Xe}@(\text{MeO})_3\text{-111}\cdot 1.5\text{DCE}$  ( $l = 8.0 \text{ \AA}$ ,  $\theta = 54(1)^\circ$ ,  $V_c \approx 53 \text{ \AA}^3$ ). No disorder is present and the conformation of the host is nearly identical to the (35%) minor occupancy conformation observed in crystals of  $(\text{MeO})_3\text{-111}\cdot 1.5\text{DCE}$ . (c) Overlay of the cryptophane cores  $\text{Xe}@(\text{MeO})_3\text{-111}$  (blue) and  $(\text{MeO})_3\text{-111}$  (red, major occupancy conformer).

#### 5.4. $(\text{MeO})_3\text{-111}\cdot 1.5\text{DCE}$ and $0.92\text{Xe}@(\text{MeO})_3\text{-111}\cdot 1.5\text{DCE}$

Crystals of  $(\text{MeO})_3\text{-111}\cdot 1.5\text{DCE}$  are a racemate. The asymmetric unit contains a single enantiomer of  $(\text{MeO})_3\text{-111}$  and one and a half molecules of DCE. Therefore,  $Z = 4$  with respect to  $(\text{MeO})_3\text{-111}$ . The cryptophane core exhibits disorder with respect to one of the arene rings and the associated  $-\text{OCH}_2\text{O}-$  bridge; see Fig. S15. The arene and bridge occupy two positions or conformations, one in which the bridge has a torsion angles ( $\tau$ ) of  $177.3^\circ$  and  $179.3^\circ$ , another in which the angles are  $82.1^\circ$  and  $172.5^\circ$  with relative occupancies converging to 65% and 35% respectively; see Table S3. This can be interpreted as the cryptophane within the crystal existing in two conformations, either closed (occupancy of 65%) resulting in a cavity volume of  $41 \text{ \AA}^3$ , or slightly expanded (occupancy of 35%). Using the SQUEEZE subroutine of

PLATON, four solvent accessible voids per unit cell were found. These sites are centered at the cavities of the cryptophane, with  $< 1$  electron per site. This implies that the cavities of the cryptophanes are essentially guest-free. A thermal ellipsoid plot of the asymmetric unit of the modeled structure is shown in Fig. S14a. CCDC deposition number for  $(\text{MeO})_3\text{-111}\cdot 1.5\text{DCE}$  is 935199.

The single crystal structure of  $0.92\text{Xe}@(\text{MeO})_3\text{-111}\cdot 1.5\text{DCE}$  is iso-structural with  $(\text{MeO})_3\text{-111}\cdot 1.5\text{DCE}$  except for a single Xe atom centered within the cavity of each  $(\text{MeO})_3\text{-111}$  with a site occupancy factor (sof) that refines to 0.92. This resulted in a more expanded cavity ( $V_c \approx 53 \text{ \AA}^3$ ) due to subtle differences in  $\tau$  angles of the  $\text{ArOCH}_2\text{OAr}$  bridges compared to the empty structure. It should be noted that there exists no positional disorder of any bridge as was observed in the  $(\text{MeO})_3\text{-111}\cdot 1.5\text{DCE}$  crystal structure. This implies that by xenon occupying the cavity, the disorder is resolved by forcing the cryptophane into the slightly more open conformation, though the conformation is intermediate with respect to the empty  $[(\text{Cp}^*\text{Ru})_6\mathbf{111}]^{6+}$  and  $0.75\text{H}_2\text{O}@111$  structures. A thermal ellipsoid plot of the asymmetric unit of the modeled structure is shown in Fig. S14b. CCDC deposition number for  $0.92\text{Xe}@(\text{MeO})_3\text{-111}\cdot 1.5\text{DCE}$  is 1027977.

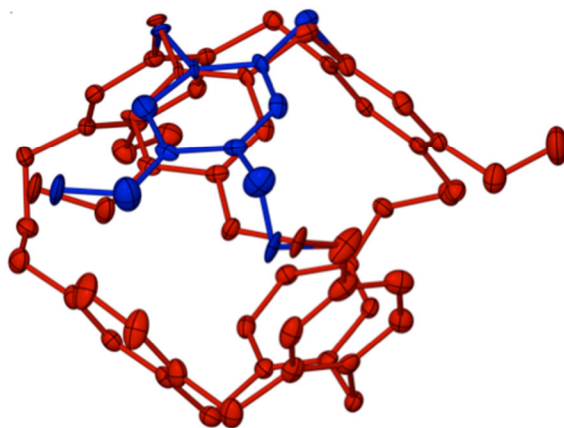


**Figure S15.** Thermal ellipsoid plot (55% probability) of the host in  $(\text{MeO})_3\text{-111}\cdot 1.5\text{DCE}$ , showing the more open conformation in blue (sof = 35%) and the closed conformation in red (sof = 65%). The solvent molecules and hydrogen atoms were omitted for clarity.

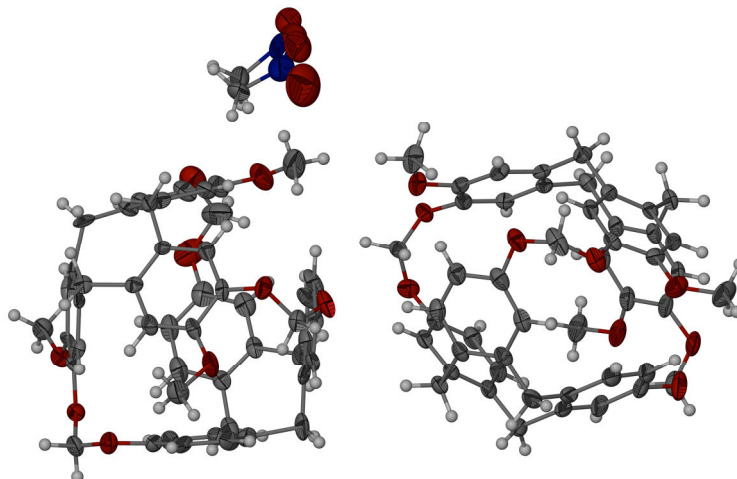


**Figure S16.** Thermal ellipsoid plots of  $1.5[(\text{MeO})_3\text{-111}]\cdot\text{NO}_2\text{Me}$  ( $l = 7.7 \text{ \AA}$ ,  $\theta = 56(2)^\circ$ ,  $V_c \approx 42 \text{ \AA}^3$ ) at 60% probability.

### 5.5. $1.5[(\text{MeO})_3\text{-111}]\cdot\text{NO}_2\text{Me}$ .

The asymmetric unit in this structure contains one and a half molecules of **(MeO)<sub>3</sub>-111** and a disordered (65:35) molecule of  $\text{NO}_2\text{Me}$  (Figure S16). One of the cryptophanes in the asymmetric unit is disordered around an inversion center, which generates the other enantiomer. A thermal ellipsoid plot of the asymmetric unit of the disorder model is shown in Figure S17. The difference Fourier map of the cryptophane shows that the cavity is essentially guest-free with electron density  $\leq 1e^- \text{ \AA}^{-3}$ . CCDC deposition number of  $1.5[(\text{MeO})_3\text{-111}]\cdot\text{NO}_2\text{Me}$  is 1027976.

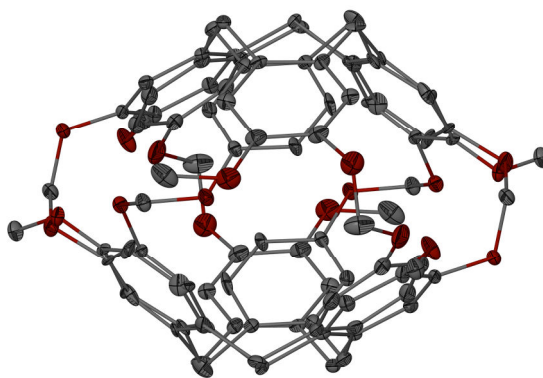


**Figure S17.** Thermal ellipsoid plots (at 30% probability) of the disordered cryptophane observed in the crystal structure of  $1.5[(\text{MeO})_3\text{-111}]\cdot\text{NO}_2\text{Me}$ .

**Table S1.** Summary of crystallography data for the different SCXR structures of **(MeO)<sub>3</sub>-111**.

Compound	<b>(MeO)<sub>3</sub>- 111</b> ·1.5DCE	0.92Xe@ <b>(MeO)<sub>3</sub>- 111</b> ·1.5DCE	1.5[ <b>(MeO)<sub>3</sub>- 111</b> ]·NO <sub>2</sub> Me
Formula	C <sub>51</sub> H <sub>48</sub> Cl <sub>3</sub> O <sub>9</sub>	C <sub>51</sub> H <sub>48</sub> Cl <sub>3</sub> O <sub>9</sub> Xe <sub>0.92</sub>	C <sub>73</sub> H <sub>66</sub> NO <sub>15.50</sub>
Formula wt. (g·mol <sup>-1</sup> )	911.24	1032.04	1205.27
Wavelength (Å)	0.71073	0.71073	0.71073
Crystal System	monoclinic	monoclinic	monoclinic
Space Group	<i>P</i> 2 <sub>1</sub> / <i>c</i>	<i>P</i> 2 <sub>1</sub> / <i>c</i>	<i>P</i> 2 <sub>1</sub> / <i>c</i>
Color	colorless	colorless	colorless
Crystal dimensions (mm <sup>3</sup> )	0.56 × 0.38 × 0.34	0.17 × 0.06 × 0.02	0.65 × 0.45 × 0.09
<i>a</i> (Å)	19.8657(19)	19.9358(2)	10.5024(14)
<i>b</i> (Å)	10.6594(10)	10.94100(10)	29.658(4)
<i>c</i> (Å)	21.676(2)	19.9358(2)	19.900(3)
α (°)	90	90	90
β (°)	109.9410(10)	107.3330(10)	102.954(2)
γ (°)	90	90	90
<i>V</i> (Å <sup>3</sup> )	4314.8(7)	4387.87(9)	6040.7(14)
<i>T</i> (K)	100(2)	100(2)	100(2)
<i>Z</i>	4	4	4
ρ <sub>calc</sub> (g·cm <sup>-3</sup> )	1.403	1.562	1.325
<i>F</i> <sub>000</sub>	1908	2107	2540
Reflections collected	31805	49839	53038
Unique reflections	9498	10591	14414
<i>R</i> (int)	0.0512	0.0463	0.0458
<i>R</i> <sub>1</sub> / <i>wR</i> <sub>2</sub> [ <i>I</i> > 2σ( <i>I</i> )]	0.0459, 0.1280	0.0337, 0.0836	0.0507, 0.1402
Goof	1.056	0.979	1.095
μ (mm <sup>-1</sup> )	0.273	0.968	0.093

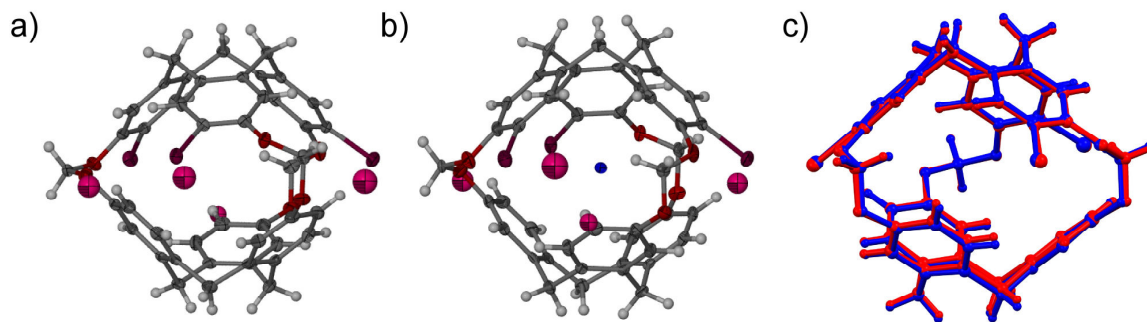


**Figure S18.** Thermal ellipsoid plots (60% probability) of the crystal structures (a) **Br<sub>3</sub>-111** ( $\tau = 107(46)^\circ$ ,  $l = 7.7 \text{ \AA}$ ,  $\theta = 51(3)^\circ$ ,  $V_c \approx 46 \text{ \AA}^3$ ) for major positions of disorder species), (b) **Xe@Br<sub>3</sub>-111** ( $\tau = 130(51)^\circ$ ,  $l = 7.9 \text{ \AA}$ ,  $\theta = 52(3)^\circ$ ,  $V_c \approx 52 \text{ \AA}^3$ ). (c) Overlay of the cryptophane cores **Xe@Br<sub>3</sub>-111** (blue) and **Br<sub>3</sub>-111**(red).

### 5.6. **Br<sub>3</sub>-111** and **Xe@Br<sub>3</sub>-111**

The crystal structure of **Br<sub>3</sub>-111** is a solvent-free racemate. The asymmetric unit contains a single enantiomer of **Br<sub>3</sub>-111**. Residual electron density ( $\geq 1e^- \text{ \AA}^{-3}$ ) was found near the rim C-H positions of the non-functionalized **CTB** moiety (Figure S18a). Multiple crystals were analyzed and the residual electron density consistently appeared in each structure, in the same locations. The residual electron density peaks were interpreted as being associated with the presence of a small amount ( $\sim 1.8\%$ , bromine positions refined) of the **Br<sub>6</sub>-111** impurity in the crystal. The magnitude of, the locations of, and distances between the electron density peaks are consistent with such an interpretation.  $^1\text{H}$  NMR also shows  $\sim 2\%$  of **Br<sub>6</sub>-111** and the species was detected in the crude reaction mixture by ESI-MS. The crystal is therefore considered to be a solid solution of  $\sim 98.2\%$  **Br<sub>3</sub>-111** and  $\sim 1.8\%$  **Br<sub>6</sub>-111**. Using the SQUEEZE subroutine of PLATON, four accessible voids were found per unit cell (**Br<sub>6</sub>-111** ignored). These sites are centered at the cavity of the cryptophane, with  $\leq 1$  electron per site. This implies that the cavities of the cryptophanes are essentially empty. CCDC deposition number for **Br<sub>3</sub>-111** is 1027974.

The single crystal structure of  $0.96\text{Xe@Br}_3\text{-111}$  is iso-structural with **Br<sub>3</sub>-111** except that a single xenon atom is centered within the cavity of each **Br<sub>3</sub>-111** with a site occupancy factor (sof) that refines to 0.96. This results in a slightly more expanded cavity ( $V_c \approx 51 \text{ \AA}^3$ ) compared to empty **Br<sub>3</sub>-111** ( $V_c \approx 46 \text{ \AA}^3$ ). A thermal ellipsoid plot of the asymmetric unit of the modeled structure is shown in Fig. S18b. CCDC deposition number for  $0.96\text{Xe@Br}_3\text{-111}$  is 1027975.

**Table S2.** Summary of crystallographic data for the different Crystal structures of **Br<sub>3</sub>-111**.

Compound	<b>Br<sub>3</sub>-111</b>	<b>0.96Xe@Br<sub>3</sub>-111</b>
Formula	C <sub>45</sub> H <sub>32.94</sub> Br <sub>3.06</sub> O <sub>6</sub>	C <sub>45</sub> H <sub>32.94</sub> Br <sub>3.06</sub> O <sub>6</sub> Xe <sub>0.96</sub>
Formula wt. (g·mol <sup>-1</sup> )	913.78	1039.83
Wavelength (Å)	0.71073	0.71073
Crystal System	monoclinic	monoclinic
Space Group	P2 <sub>1</sub> /n	P2 <sub>1</sub> /n
Color	colorless	colorless
Crystal dimensions (mm <sup>3</sup> )	0.26 0.26 × 0.24	0.12 × 0.10 × 0.07
<i>a</i> (Å)	10.6375(10)	10.85910(10)
<i>b</i> (Å)	30.647(3)	30.5071(4)
<i>c</i> (Å)	11.2147(10)	11.08070(10)
α (°)	90	90
β (°)	95.9160(10)	94.2160(10)
γ (°)	90	90
<i>V</i> (Å <sup>3</sup> )	3636.6(6)	3660.88(7)
<i>T</i> (K)	100(2)	100(2)
<i>Z</i>	4	4
ρ <sub>calc</sub> (g·cm <sup>-3</sup> )	1.669	1.887
<i>F</i> <sub>000</sub>	1831	2039
Reflections collected	28012	26976
Unique reflections	8291	8852
<i>R</i> (int)	0.0453	0.0453
<i>R</i> <sub>1</sub> / <i>wR</i> <sub>2</sub> [ <i>I</i> > 2σ( <i>I</i> )]	0.0383, 0.0895	0.0341, 0.0759
Goof	1.034	1.040
μ (mm <sup>-1</sup> )	3.441	4.293

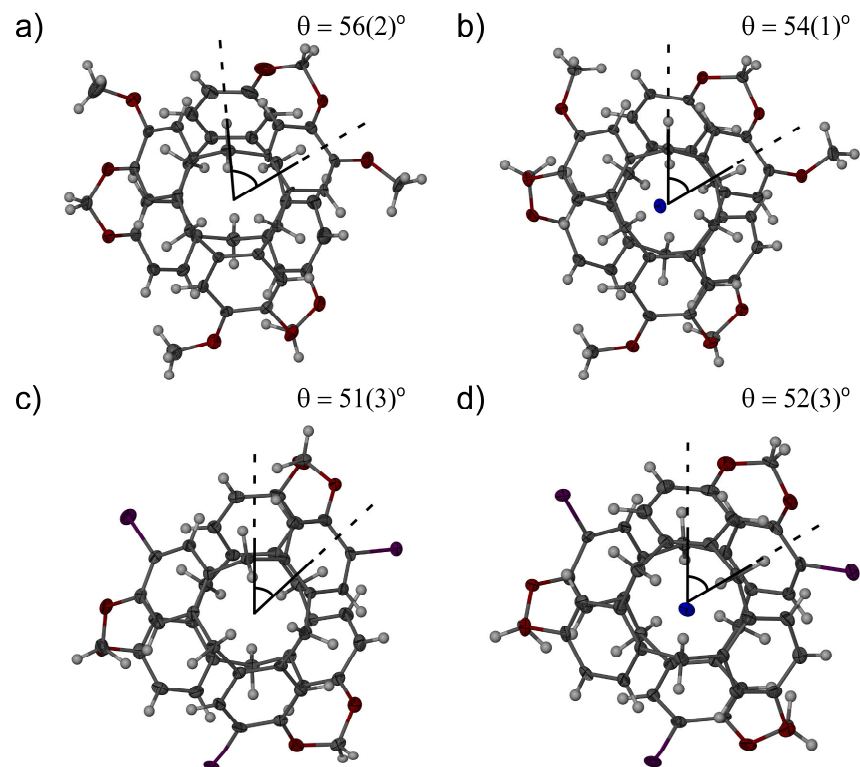


**Figure S19.** Thermal ellipsoid plots of (a)  $(\text{MeO})_3\text{-111}$  from the crystal structure of  $(\text{MeO})_3\text{-111}\cdot 1.5\text{DCE}$ , (b)  $0.92\text{Xe}@(\text{MeO})_3\text{-111}$  from the crystal structure of  $0.96\text{Xe}@(\text{MeO})_3\text{-111}\cdot 1.5\text{DCE}$ , (c)  $\text{Br}_3\text{-111}$  from the crystal structure of  $\text{Br}_3\text{-111}$ , and d)  $0.96\text{Xe}@(\text{Br}_3\text{-111})$  from the crystal structure of  $0.96\text{Xe}@(\text{Br}_3\text{-111})$ , at 60% probability showing the twist angles. Only one enantiomer of each and the major occupancy positions of disordered species are shown.

**Table S3.** Analysis of  $C_{Ar}-C_{Ar}-O-CH_2$  dihedral angles ( $\tau$ ) of **R<sub>3</sub>-111** structures, as defined by Scheme 1. “Top” refers to the CTB cup with the **R** group.

<b>R<sub>3</sub>-111</b> in ASU of crystal structure	$\tau^\circ_{top}$	Conformation	$\tau^\circ_{bottom}$	Conformation
1.5[( <b>MeO</b> ) <sub>3</sub> - <b>111</b> ] $\cdot$ NO <sub>2</sub> Me				
( <b>MeO</b> ) <sub>3</sub> - <b>111</b> ordered	165.6	+antiperiplanar	77.6	+synclinal
	-174.5	-antiperiplanar	169.4	-antiperiplanar
	-130.9	-anticlinal	61.4	+synclinal
( <b>MeO</b> ) <sub>3</sub> - <b>111</b> disordered	156.4	+antiperiplanar	74.9	+synclinal
	-170.5	-antiperiplanar	-168.6	-antiperiplanar
	-130.3	-anticlinal	64.8	+synclinal
0.92Xe@( <b>MeO</b> ) <sub>3</sub> - <b>111</b> $\cdot$ 1.5DCE				
0.92Xe@( <b>MeO</b> ) <sub>3</sub> - <b>111</b>	82.4	+synclinal	158.2	+antiperiplanar
	64.8	+synclinal	146.8	+anticlinal
	173.6	-antiperiplanar	-172.2	-antiperiplanar
( <b>MeO</b> ) <sub>3</sub> - <b>111</b> $\cdot$ 1.5DCE				
More open conformer 35% bridge	82.1	+synclinal	172.5	+antiperiplanar
More closed conformer 65% bridge	-177.3	-antiperiplanar	-179.3	-antiperiplanar
	-170.4	-antiperiplanar	-176.0	-antiperiplanar
	69.0	+synclinal	138.9	+anticlinal
<b>Br<sub>3</sub>-111</b>				
	145.8	+anticlinal	63.5	+synclinal
	148.7	+anticlinal	73.1	+synclinal
	-174.3	+antiperiplanar	-176.4	-antiperiplanar
0.96Xe@ <b>Br<sub>3</sub>-111</b>				
	-148.3	+anticlinal	-66.3	+synclinal
	-147.7	+anticlinal	-69.1	+synclinal
	174.9	+antiperiplanar	178.0	+antiperiplanar

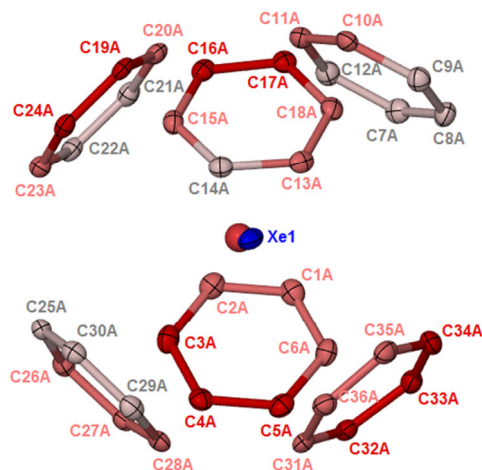


**Figure S20.** Thermal ellipsoids at 60% probability of the phenyl carbons and xenon in the cryptophane cavity of  $0.92\text{Xe}@\text{(MeO)}_3\text{-111}\cdot 1.5\text{DCE}$ . The colors are based on the distances between the phenyl carbons and xenon, 0 – 3.800 Å are red, 3.801 – 4.000 Å are pink and 4.001+ Å are light pink. The red solid sphere at the center of the cavity is the centroid of all the phenyl carbons. It is located 0.23 Å from the xenon position.

**Table S4.** Xe $\cdots$ C(arene) intermolecular contacts in  $0.92\text{Xe}@\text{(MeO)}_3\text{-111}\cdot 1.5\text{DCE}$  structure. See Fig. S20 above for carbon labels.

C(arene)	Xe $\cdots$ C distance / Å	C(arene)	Xe $\cdots$ C distance / Å
C16A	3.640	C2A	3.844
C17A	3.662	C1A	3.847
C19A	3.679	C36A	3.886
C4A	3.701	C11A	3.891
C32A	3.707	C26A	3.896
C5A	3.712	C13A	3.946
C33A	3.729	C28A	3.977
C24A	3.756	C23A	3.994
C3A	3.770	C14A	4.007
C34A	3.788	C9A	4.036
C31A	3.802	C25A	4.063
C18A	3.803	C21A	4.098
C6A	3.815	C12A	4.149
C10A	3.821	C22A	4.192
C35A	3.825	C29A	4.212
C20A	3.836	C30A	4.254
C15A	3.837	C8A	4.305
C27A	3.838	C7A	4.346
Average = 3.91(19) Å			

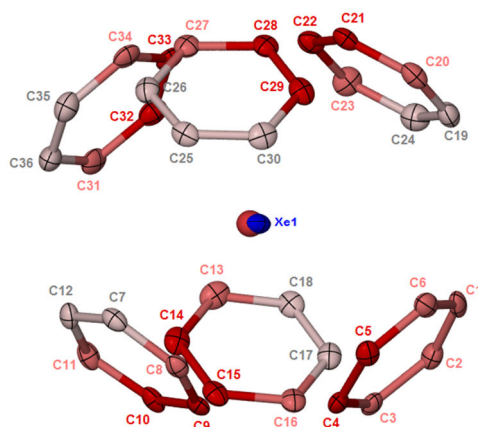


**Figure S21.** Thermal ellipsoids plot at 60% probability of the phenyl carbons and xenon in the cryptophane cavity of  $0.96\text{Xe}@Br_3\text{-111}$ . The colors are based on the distances from the between the phenyl carbons and xenon, 0 – 3.800 Å are red, 3.801 – 4.000 Å are pink and 4.001+ Å are light pink. The red solid sphere at the center of the cavity is the centroid of all the phenyl carbons. It is located 0.14 Å from the xenon position.

**Table S5.**  $\text{Xe}\cdots\text{C}(\text{arene})$  intermolecular contacts in  $0.96\text{Xe}@Br_3\text{-111}$ . See above figure for carbon labels.

C(arene)	Xe $\cdots$ C distance /Å	C(arene)	Xe $\cdots$ C distance /Å
C21	3.665	C27	3.866
C10	3.667	C1	3.902
C28	3.679	C2	3.928
C15	3.695	C23	3.944
C33	3.697	C8	3.947
C22	3.704	C31	3.947
C4	3.705	C13	3.955
C9	3.727	C35	4.008
C5	3.731	C30	4.015
C29	3.739	C12	4.048
C32	3.755	C17	4.067
C14	3.759	C7	4.076
C3	3.813	C36	4.08
C34	3.82	C19	4.086
C6	3.832	C18	4.105
C11	3.846	C26	4.133
C16	3.850	C24	4.139
C20	3.855	C25	4.202

Average = 3.89(16)

**Table S6.** Xe...centroid(arene) distances from the structures of 0.92Xe@(**MeO**)<sub>3</sub>-**111**·1.5DCE and 0.96Xe@**Br**<sub>3</sub>-**111**.

<b>Label</b>	<b>Xe...centroid(arene) distance /Å</b>
<b>(MeO)<sub>3</sub>-111</b>	
1	3.52
2	3.53
3	3.55
4	3.68
5	3.80
6	3.85
Average	3.65(14)
<b>Br<sub>3</sub>-111</b>	
1	3.56
2	3.63
3	3.63
4	3.65
5	3.65
6	3.69
Average	3.63(4)

## 6. References

- S1. H. M. Strohalm M., Kořata B., Kodíček M. , *M. Rapid Commun. Mass. Spec.*, 2008, **6**, 905-908.
- S2. T. Traore, G. Clave, L. Delacour, N. Kotera, P. Y. Renard, A. Romieu, P. Berthault, C. Boutin, N. Tassali and B. Rousseau, *Chem. Commun.*, 2011, **47**, 9702-9704.
- S3. M. Little, J. Donkin, J. Fisher, M. Halcrow, J. Loder and M. Hardie, *Angew. Chemie Int. Ed.*, 2012, **51**, 764-766.
- S4. J. Canceill and A. Collet, *New J. Chem.*, 1986, 17-23.
- S5. J. Canceill, J. Gabard and A. Collet, *J. Chem. Soc., Chem. Commun.*, 1983, 122-123.
- S6. C. Landon, P. Berthault, F. Vovelle and H. Desvaux, *Protein Sci.*, 2001, **10**, 762-770.
- S7. P. Berthault, G. Huber and H. Desvaux, *Prog. NMR Spectrosc.*, 2009, 35-60.
- S8. G. Sheldrick, *Acta Crystallogr., Sect. A: Found. Crystallogr.*, 2008, **64**, 112-122.
- S9. L. J. Barbour, *Supramol. Chem.*, 2001, **1**, 189-191.